Macromolecules

ARTICLE

pubs.acs.org/Macromolecules

Theory of Yielding, Strain Softening, and Steady Plastic Flow in Polymer Glasses under Constant Strain Rate Deformation

Kang Chen[†,*] and Kenneth S. Schweizer[*,‡]

[†]Center for Soft Condensed Matter Physics and Interdisciplinary Research, Soochow University, Suzhou 215006, China

[‡]Department of Materials Science, University of Illinois, 1304 West Green Street, Urbana, Illinois 61801, United States

ABSTRACT: The nonlinear Langevin equation theory of segmental relaxation, elasticity, and nonlinear mechanical response of deformed polymer glasses with aging and mechanical rejuvenation processes taken into account is applied to study material response under a constant strain rate deformation. In the postyield softening regime, the amplitude of the stress overshoot feature, and its breadth in strain, are predicted to be positively correlated with the mechanically induced disordering process. The key physics is the increase of the density fluctuation amplitude due to mechanically generated disorder (rejuvenation) which reduces the elastic modulus and speeds up relaxation beyond the effects of the landscape tilting mechanism. Detailed numerical calculations reveal that the emergence of strain softening is not directly tied to a difference between the initial and steady plastic flow states, but rather on whether there exists a rejuvenation-dominated process during deformation. Calculations suggest a roughly linear relation between the strain softening amplitude (SSA) and the amount of rejuvenation as quantified by variation of the density fluctuation amplitude. The dependences of the yield stress and strain, steady state flow stress, and SSA on deformation rate, temperature, preaging time, and also two distinct thermal history protocols are investigated in detail for PMMA glass. Overall, good agreement between theory and experiment is found.

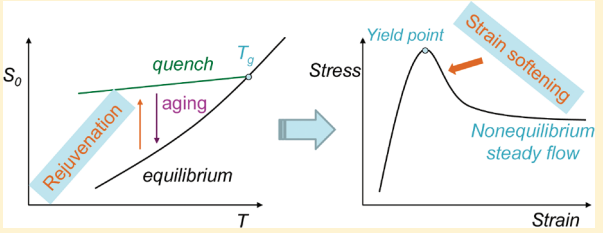

I. INTRODUCTION

Polymer glasses are ubiquitous "thermoplastic" materials that are widely employed in industry and daily life. Fundamental understanding of their ultraslow nonequilibrium dynamics and nonlinear mechanical properties remains a challenging problem.[1−5] The glassy alpha relaxation process occurs on the local "statistical segment" (∼nanometer) scale and sets the elementary time scale for a hierarchy of relaxation processes associated with cooperative intrachain motions that extend to the macromolecular scale.[6] Recent experiments and simulations have revealed an intimate coupling between macroscopic nonlinear mechanical response and the local segmental relaxation in polymer glasses.[7−11] Moreover, the dynamics on the segmental scale is very nearly isotropic even under strong uniaxial deformation conditions.[12,13] These simplifications provide strong motivation for the theoretical approach employed in the present study.[14,15]

Upon external deformation, the segmental relaxation time can be greatly reduced, resulting in irreversible local "plastic flow" or "dynamic yielding". In a constant deformation rate experiment, there are typically five strain amplitude regime:[3−5] (i) linear stress growth in the low strain elastic regime, (ii) beyond a strain of a few percent there is an "anelastic" regime where stress increases more slowly than linearly, (iii) a local stress maximum at the so-called "yield peak", followed by a drop of the stress with strain known as "strain softening", (iv) a plastic flow regime characterized by a (nearly) constant plateau stress indicative of irreversible activated motion on a local segmental scale,[14,15] and (v) at large enough deformation the material either fails or the stress increases strongly due to chain deformation and "strain hardening".[4,16−23] A "flat" flow stress in regime iv is often not observed, in which case a flow stress is operationally defined as the local minimum which separates the strain softening and hardening regimes. A fundamental understanding of the competition between strain softening and strain hardening is of high practical importance since it determines material failure properties such as crazing, necking, or shear banding.[3−5] At strains in the plastic flow regime and beyond, the thermal history and physical aging effects are "erased", corresponding to a nonequilibrium steady state. However, the mechanical and relaxation responses in regimes i−iii depend on thermal history.

Monte Carlo simulations of simple tangent bead−spring models of amorphous polymer glasses have found strain softening arises from a drop of interchain contributions to stress.[24] Experiments by Halary, Monnerie, and co-workers reveal a close correlation between strain softening and the issue of whether physical aging effects are, or are not, operative.[25−27] For example, the amplitude of the stress overshoot tends to vanish when the highly local beta process motions are the precursors of the alpha relaxation (e.g., unaged poly(methyl methacrylate) (PMMA)) but becomes large when the beta process involves only isolated motions (e.g., aged PMMA).[25−27] Phenomenologically, many experiments on diverse polymeric materials[3,19,28−30] have shown

Received: February 24, 2011
Revised: April 17, 2011
Published: May 03, 2011

(i) the strain softening amplitude (SSA), defined as the magnitude of the stress overshoot, grows roughly logarithmically with waiting (aging) time and deformation rate, (ii) a rapid thermal quench or predeformation can largely or entirely eliminate the stress overshoot and yield peak, (iii) physical aging restores softening for both thermally and mechanically pretreated glasses, and (iv) annealed and quenched glasses have an identical flow stress and hardening response. These phenomena are believed to be a consequence of so-called "mechanical rejuvenation", sometimes interpreted as a literal "erasure of aging", but more generically viewed as the effect of mechanical disordering of one or more key structural variables.[2,3] At low strains ("pre-yield" regime), aging, thermal history, and mechanical response are coupled. However, at large ("post-yield") strains, aging and thermal history are "erased", and a nonequilibrium steady state is achieved.

Recently, we have developed a nonlinear Langevin equation (NLE) theory of the segmental relaxation, elasticity, and mechanical response of polymer glasses under rapid quench conditions where aging and rejuvenation do not affect the mechanical properties.[15] Most recently, this theory has been extended to describe the coupled effects of physical aging, mechanical rejuvenation, and thermal history, and a few consequences relevant to creep experiments and attainment of a long time steady state in the absence of strain hardening have been worked out.[31] Mechanically generated disorder (rejuvenation) is quantified by a dissipative work argument where deformation increases the amplitude of density fluctuations that is the key structural variable of the theory, corresponding to driving the material up the potential energy landscape (PEL). This disorder-induced production of density fluctuations competes with the opposite effect of physical aging which pushes the system down the PEL toward equilibrium and reduces density fluctuations. As discussed in detail in our most recent work,[31] mechanical enhancement of the dimensionless density fluctuation amplitude has been directly observed in a small-angle scattering experiment.[32] This provides direct support for our idea to use this observable quantity as the relevant structural variable. Although we are unaware of any experiments that directly address the question of whether the density fluctuation amplitude decreases with aging, this seems inevitable since aging corresponds to an approach to equilibrium down the potential energy landscape. Moreover, our prior theoretical predictions of physical aging based on this idea agree well with experiments.[33,34]

The goal of the current paper is to apply the new theory[31] (in the absence of hardening) to constant strain rate measurements and construct a physical picture for the physics of strain softening and how preaging, aging during deformation, and mechanical disordering combine to determine the experimental yield stress and strain. In this first study, the focus is on establishing the many trends we predict and qualitative comparisons with experiments to provide sensibility checks. Detailed quantitative numerical comparisons with experimental data for specific polymer glasses will be pursued in the future.

In section II we summarize relevant aspects of prior work and its generalization to treat a constant strain rate measurement. Model calculations are presented in section III that establish how stress, relaxation time, and density fluctuation amplitude evolve with increasing strain for a range of temperatures, deformation rates, and preaging times. A detailed model study of the SSA is also presented. Section IV studies the plastic flow regime and attainment of a nonequilibrium steady state, and brief comparisons with experiment and simulations are performed. The paper concludes in section V with a summary.

II. THEORETICAL BACKGROUND

The NLE theory of glassy segmental relaxation, quiescent physical aging, and nonlinear mechanical response under rapid quench conditions has been discussed in detail[14,15,23,33−36] and extensively reviewed in two recent articles.[37,38] The reader is referred to these earlier papers for an in-depth discussion of the theoretical basis of the approach. Here, we only summarize the key elements of the theory and our recent extension to treat coupled physical aging and mechanical disordering effects.[31]

A. Quiescent Relaxation, Elasticity, and Aging. NLE theory is formulated at the level of modestly coarse-grained statistical segments representing a collection of a few monomer units of size $\sigma = C_\infty^{1/2} l_b$, where l_b is the backbone chemical bond length and $C_\infty \sim 4-10$ the characteristic ratio. The slow alpha relaxation process in the deeply supercooled and glass regimes is described by a stochastic nonlinear Langevin equation[39,40]

$$\zeta_s \frac{\partial r_\alpha(t)}{\partial t} = -\frac{\partial F_{eff}[r_\alpha(t)]}{\partial r_\alpha(t)} + \delta f_\alpha(t) \quad (1)$$

where $r_\alpha(t)$ is the absolute value of the displacement of segment α from its initial position. The very local and fast (intrasegment scale) motions are embedded in the short time friction constant, ζ_s, and the white-noise random force which satisfies $\langle \delta f_\alpha(0) \delta_\alpha f(t) \rangle = 2k_B T \zeta_s \delta(t)$. The associated fast relaxation time scale is modeled as a noncooperative Arrhenius process, $\tau_0(T) \equiv \tau_0 \exp(\varepsilon_A / k_B T)$, where $\tau_0 \approx 10^{-14\pm1}$ s is a vibrational time scale and ε_A the local activation energy.[38,41] The "dynamic free energy" quantifies caging constraints and determines the transient localization length and activation barrier. It is given by

$$\beta F_{eff}(r) = -3\ln(r) - \int \frac{d\vec{q}}{(2\pi)^3} \rho C^2(q) S(q) [1 + S(q)]^{-1} \exp\left\{ -\frac{q^2 r^2}{6} [1 + S^{-1}(q)] \right\} \quad (2)$$

where $\beta \equiv (k_B T)^{-1}$ is the inverse thermal energy. A Gaussian thread model for the required structural correlations in eq 2 is adopted corresponding to preaveraging subnanometer structural and interaction details. The resulting site−site direct correlation function $C(q) = C(q=0) = C_0$, and the collective density fluctuation structure factor is $S^{-1}(q) = S_0^{-1} + (1/12) q^2 \sigma^2$, where $S_0 = \rho k_B T \kappa = (-\rho C_0)^{-1}$ is the dimensionless isothermal compressibility (above T_g in equilibrium) that quantifies the amplitude of density fluctuations on nanometer and beyond scales, κ the isothermal compressibility, and $\rho\sigma^3$ the reduced segmental density. Theory and experiment suggest $S_0^{-1/2} = -A + (B/T)$, where $A > 0$ and B are experimentally known, and the latter correlates with monomer cohesive energy.[40,41] Substituting these relations in eq 2, $F_{eff}(r)$ for long chains is determined by a single dimensionless material-specific "coupling constant"

$$\lambda \equiv (\rho \sigma^3 S_0^{3/2})^{-1} \quad (3)$$

which increases with cooling or pressure and involves only measurable quantities.

Equations 1−3 predict a dynamical crossover (also known as the naïve mode coupling theory ideal glass transition[38,42]) at $\lambda_c = 8.32$ where a local minimum (at a localization length, r_{loc}) and barrier

(height, F_B) emerge in the dynamic free energy at $T_c = B[A + (\lambda_c \rho\sigma^3)^{1/3}]^{-1} > T_g$.[40,41] The analytic version of NLE theory employed here is based on the mean barrier hopping or alpha time, $\tau_\alpha(T)$, modeled in a Kramers-like manner as[40]

$$\tau_\alpha(T) = \tau_0 \exp\left(\frac{\varepsilon_A}{k_B T}\right) \exp\left[\frac{a_c F_B(T)}{k_B T}\right] \quad (4)$$

The local activation energy is determined by adopting the recent observation[43] of a (nearly) universal "magic relaxation time" at T_c: $\tau_0(T_c) \equiv \tau_0 \exp(\varepsilon_A/k_B T_c) \cong 10^{-7\pm1}$ s. Chain connectivity induces a short-range "intrachain cooperativity" of the hopping event associated with backbone stiffness, crudely modeled in eq 4 via a material-specific (but temperature-independent) parameter, a_c. This parameter reflects the number of dynamically correlated segments along the chain and has been a priori estimated to be $a_c \sim 1-8$.[41] The NLE theory predicts sensible values for T_c and T_g based on the experimental kinetic vitrification criterion $\tau_\alpha(T_g) = 10^x$ s, where $x = 2-4$.[40,41]

Extension of NLE theory to below T_g assumes the dimensionless density fluctuation amplitude, S_0, remains the relevant slow variable and quantifies the caging constraints.[35] After a rapid quench to below T_g, S_0 falls out of equilibrium, and its temperature dependence acquires a nonequilibrium form composed of two contributions: (i) $S_0 \propto T$ sufficiently far below T_g as in a harmonic solid and (ii) frozen-in density fluctuations, $S_0(T\rightarrow 0) \equiv bS_0(T_g)$, where experimentally $b \sim 0.4-0.75$. From a PEL perspective, these two contributions correspond to equilibrated (intrabasin) vibrational motions and trapped (nonequilibrium) larger scale structural rearrangements (interbasin). Hence, a minimalist form for quenched glass is suggested[35]

$$S_0(T) = bS_0(T_g) + \frac{T}{T_g}(1-b)S_0(T_g) \quad (5)$$

where the first (second) term is the contribution from the slow (fast) degrees of freedom.

In the nonequilibrium glass, the fundamental structural variable, and consequently the mean segmental relaxation time and all other viscoelastic properties, become time dependent due to physical aging. A first-order kinetic model[33,34] is employed to describe the time evolution of $S_0(t)$ from its nonequilibrium quenched value ($t = 0$) to the smaller equilibrium value, $S_{0,l}$

$$\frac{dS_0(t)}{dt} = -\frac{S_0(t) - S_{0,l}}{\tau_\alpha(t)} \quad (6)$$

The physical idea is equilibration down the PEL proceeds via activated hopping which is self-consistently determined by $S_0(t)$ via eqs 3−6. The fast local process in eq 4 is assumed to be age independent, a reasonable simplification in the sub-T_g regime.

The glassy elastic shear modulus, G', due to interchain stresses can be calculated under all conditions using the standard formula:[35,38]

$$G' = \frac{k_B T}{60\pi^2}\int_0^\infty dq \left[q^2 \frac{d}{dq}\ln(S(q))\right]^2 e^{-q^2 r_{loc}^2/3S(q)} \quad (7)$$

Young's modulus follows as $E' \simeq 2.8G'$.[15]

B. Combined Effect of Applied Stress, Mechanical Rejuvenation, and Aging. In general, glasses under stress are subject to three simultaneous and coupled nonlinear effects: forces on segments due to applied stress, structural mechanical disordering, and physical aging. The most elementary effect is that stress introduces an anisotropic bias which lowers activation barriers corresponding to a direct mechanical acceleration of relaxation. Analogous to the Eyring landscape tilting idea,[44−46] this effect is modeled[14] as an isotropic external force acting on each segment, a simple picture with simulation support.[12,47] The tilting mechanism can be viewed as stress introducing a mechanical work contribution to the dynamic free energy[14,48]

$$F_{mech}(r) = -fr, \quad f = c\sigma^2\tau \quad (8)$$

where τ is applied stress and the prefactor $c = (\pi\rho\sigma^3/6)^{-2/3}$ is of order unity and enters only as a linearly multiplicative modification of stress. Applied stress reduces the barrier and accelerates relaxation, but with multiple non-Eyring features.[14] It also increases the localization length, r_{loc}, and thereby reduces the elastic modulus (eq 7). The fast relaxation time scale, $\tau_0(T)$, is assumed to be deformation independent.

At large enough stress, mechanically induced structural disorder occurs which further enhances activated relaxation. Typically, such an effect is described by a term in the evolution equation for the structural variable that scales linearly with strain rate. In our approach, this "rejuvenation" effect is modeled via a first-order evolution equation:[31]

$$\frac{dS_0}{dt} = \psi(S_{0,g} - S_0)\tau\dot{\gamma}_{pl} \quad (9)$$

where ψ is a (a priori unknown) numerical prefactor (in units of inverse stress, $(k_B T/\sigma^3)^{-1}$), $S_{0,g}$ the freshly quenched value, and $\dot{\gamma}_{pl} = \tau/[E'(\tau)\tau_\alpha(\tau)]$ is the plastic strain rate.[15,31] The physical idea is the disorder (density fluctuation) production rate is proportional to the dissipated power, as proposed by Langer[49] which obeys the minimum constraint that the production rate is an even function of deformation rate. The freshly quenched value, $S_{0,g}$, serves as an "end point" to the rejuvenation process. Currently, there is no consensus definition for the latter; our choice is consistent with Langer,[49] who assumes the limiting reference state to be a glass with the degree of structural disorder frozen in at T_g.

As briefly discussed in our prior paper,[31] we note in passing that Langer's phenomenological "shear transformation zone" (STZ) approach postulates the key structural variable is a density of plastic zones which is controlled by an effective temperature. This picture is obviously distinct from our spatially homogeneous approach based on measurable density fluctuations which is formulated in a liquid state spirit, in contrast to the STZ, spatially inhomogeneous solid-state defect scenario.

Now, the literal rejuvenation hypothesis[2,50] does not apply at nonzero temperature where aging occurs in parallel with mechanical stirring. Under low stress preyield conditions, experiments find the aging equilibration time is unperturbed,[2] and the increase of the segmental relaxation time with aging time, and decrease with applied stress, are effectively independent or additive processes.[11] For large deformations little is fundamentally understood. We assume that the separation of aging and mechanical disordering still holds *at the level* of the evolution equation for the structural variable[31]

$$\frac{dS_0}{dt} = \psi(S_{0,g} - S_0)\tau^2/(E'(\tau, S_0)\tau_\alpha(\tau, S_0)) - (S_0 - S_{0,l})/\tau_\alpha(0, S_0) \quad (10)$$

The first (second) term on the right-hand side of eq 10 represents the contribution of mechanical disordering (aging). The relaxation time that quantifies the rejuvenation process involves

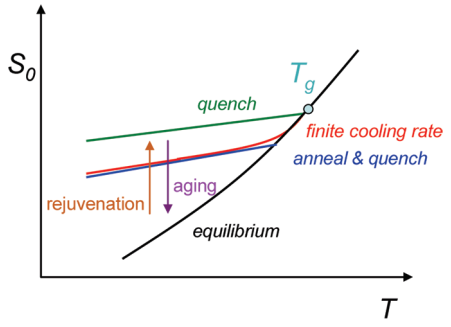

Figure 1. Schematic plot of the dimensionless density fluctuation amplitude, S_0, as a function of temperature for glasses created via different processing or thermal history routes. Quiescent aging corresponds to S_0 decreasing toward its equilibrium value, while rejuvenation is a process where S_0 increases toward its freshly quenched value.

stress-dependent activated hopping sensitive to both the mechanically driven disorder and landscape tilting aspects. On the other hand, aging is controlled by quiescent glass physics. The fast relaxation process is assumed to remain unaffected by aging and stress. The balance between aging and rejuvenation at long time determines the nonequilibrium steady state ($S_{0,\infty}$) in creep[31] and the steady flow state in constant strain rate response ($S_{0,pf}$, see section IIIA).

C. Constitutive Equation. Ignoring physical aging and mechanical rejuvenation effects, a generalized Maxwell constitutive equation has been proposed relevant to quenched conditions where the only input is the stress-dependent elastic modulus and mean segmental relaxation time[15]

$$\tau(t) = \int_0^t E(t-t')\dot{\gamma}(t')\,\mathrm{d}t' \tag{11}$$

where $\dot{\gamma}(t)$ is a time-dependent strain rate. The deformation-dependent modulus obeys

$$\frac{\mathrm{d}E[t;\tau(t)]}{\mathrm{d}t} = -\frac{E[t;\tau(t)]}{\tau_\alpha[\tau(t)]} \tag{12}$$

and hence

$$\tau(t) = \int_0^t \mathrm{d}t'\, E'[\tau(t')]\exp\{-\int_{t'}^t \mathrm{d}t''\,\tau_\alpha^{-1}[\tau(t'')]\}\dot{\gamma}(t') \tag{13}$$

or in the differential form

$$\frac{\mathrm{d}\tau}{\mathrm{d}t} = E'[\tau(t)]\dot{\gamma}(t) - \frac{\tau(t)}{\tau_\alpha[\tau(t)]} \tag{14}$$

where $E'(\tau) = 2.8G'(\tau)$ is the stress-dependent glassy elastic modulus. The form of eqs 13 and 14 are unchanged in the presence of aging and mechanical rejuvenation. The latter enters only via the time-dependent density fluctuation amplitude, $S_0(t)$, which is nonlinearly coupled with the evolution of stress or strain. Equation 14 is then modified as

$$\frac{\mathrm{d}\tau}{\mathrm{d}t} = E'[S_0(t);\tau(t)]\dot{\gamma}(t) - \frac{\tau(t)}{\tau_\alpha[S_0(t);\tau(t)]} \tag{15}$$

where $S_0(t)$ obeys eq 10 and $\tau(t)$ includes the stress-induced landscape tilting effect. Stressed versions of eqs 2, 4, 5, 10, and 15 comprise a self-consistent nonlinear description of mechanical response encompassing aging and mechanical rejuvenation effects.

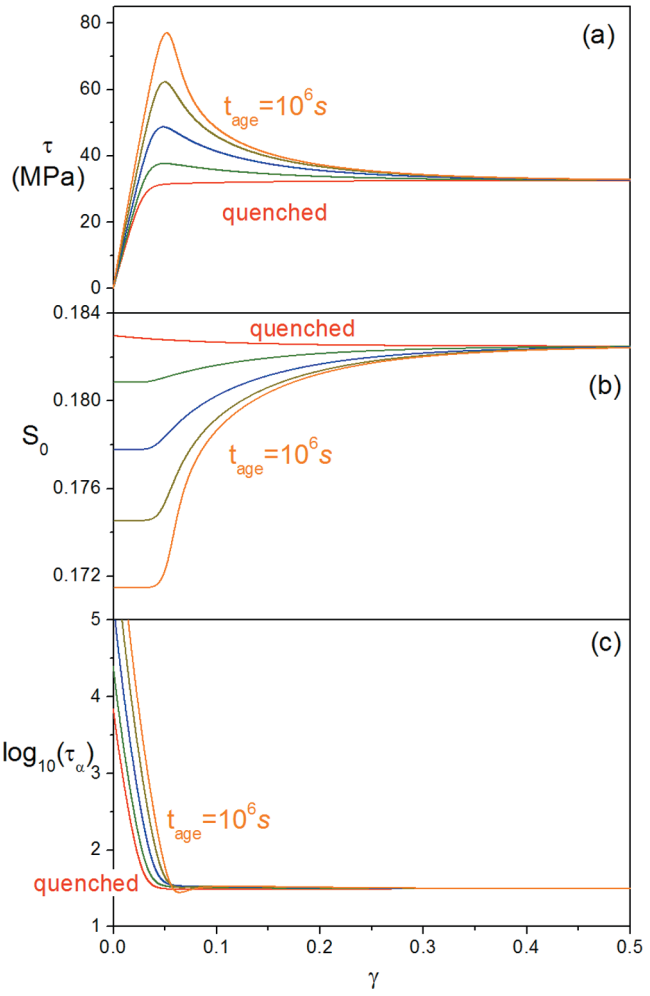

Figure 2. (a) Constant strain rate stress−strain curves for fixed $T = T_g - 30$ K and a strain rate $\dot{\gamma} = 10^{-3}\ s^{-1}$ at preaging times (bottom to top): $t_{age} = 0$(quenched), 10^3, 10^4, 10^5, and 10^6 s. The corresponding strain dependence of the dimensionless density fluctuation amplitude, S_0, and logarithmic mean relaxation time (in seconds), $\log(\tau_\alpha)$, are shown in (b) and (c), respectively. In (c), the values of $\log(\tau_\alpha)$ at zero strain for preaging times from 0 to 10^6 s are 3.85, 4.4, 5.5, 6.22, and 7.18.

For a constant deformation rate experiment, strain is $\gamma \equiv \dot{\gamma}t$. The stress−strain relation then follows from eq 15 as

$$\frac{\mathrm{d}\tau}{\mathrm{d}\gamma} = E'[S_0(t);\tau(\gamma)] - \frac{\tau(\gamma)}{\dot{\gamma}\tau_\alpha[S_0(t);\tau(\gamma)]} \tag{16}$$

At large deformation in the absence of strain hardening, the steady plastic flow state follows from the criterion $\mathrm{d}\tau/\mathrm{d}\gamma = 0$, which explicitly yields

$$\tau_{pf} = \dot{\gamma}[E'(\tau_{pf})\tau_\alpha(\tau_{pf})] \equiv \eta(\tau_{pf})\dot{\gamma} \tag{17}$$

where the final equality defines a viscosity at the Maxwell model level.

D. Model Calculations and Protocols. In the remainder of this article we apply the above constitutive equation theory under constant strain rate conditions. We address the questions of yielding, strain softening (stress drop), and plastic flow that cover

dx.doi.org/10.1021/ma200436w |*Macromolecules* 2011, 44, 3988–4000

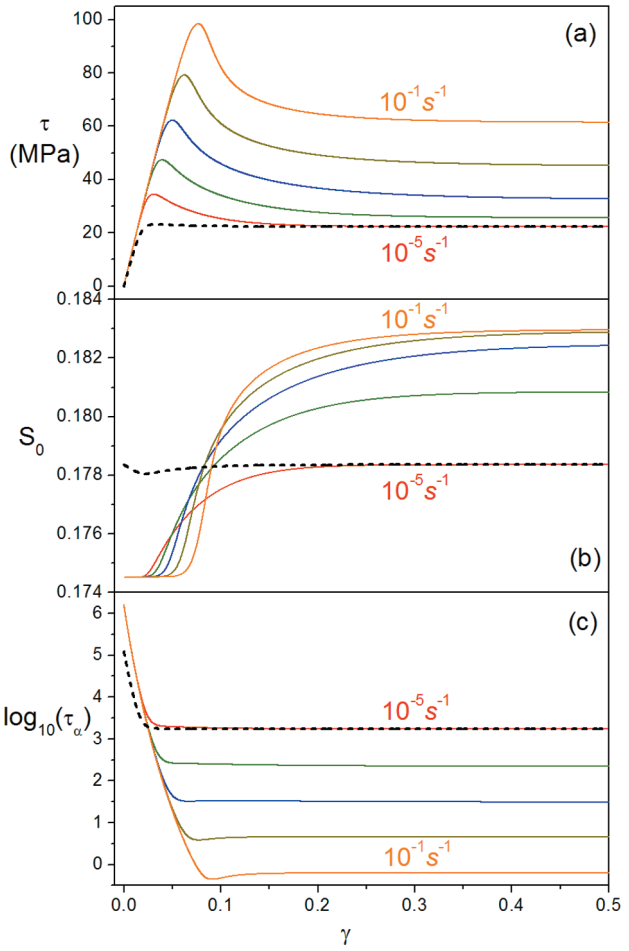

Figure 3. Same as Figure 2 but for fixed $T = T_g - 30$ K and preaging time $t_{age} = 10^5$ s at strain rates: $\dot{\gamma} = 10^{-5}$, 10^{-4}, 10^{-3}, 10^{-2}, and 10^{-1} s^{-1} (solid curves). The dashed curves are for $T = T_g - 30$ K, $\dot{\gamma} = 10^{-5}$ s^{-1} with the initial state satisfying $S_{0,i} = S_{0,pf}$ (see main text).

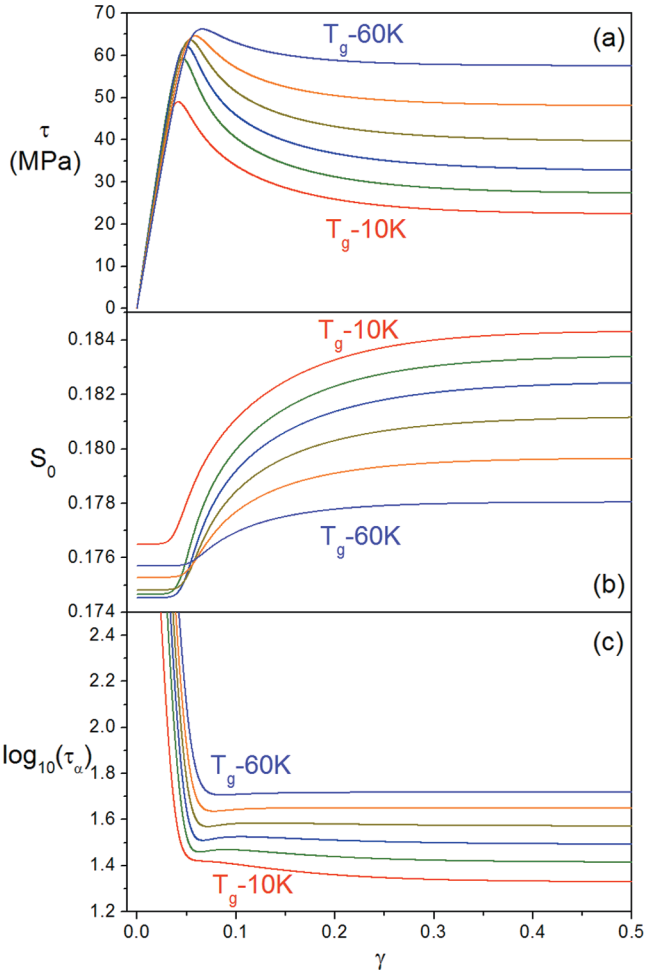

Figure 4. Same as Figure 2 but for fixed preaging time $t_{age} = 10^5$ s and strain rate $\dot{\gamma} = 10^{-3}$ s^{-1} at variable temperatures of $T = T_g - 10$ K, $T_g - 20$ K, $T_g - 30$ K, $T_g - 40$ K, $T_g - 50$ K, and $T_g - 60$ K. In (c), the values of $\log(\tau_\alpha)$ at zero strain for temperatures from $T_g - 10$ K to $T_g - 60$ K are 5.16, 5.94, 6.22, 6.38, 6.51, and 6.67.

the deformation regime beyond the "yield peak" (typically ~5−10% strain) under the simplification that strain hardening is absent. All computations are performed for a single set of material parameters developed[15] for PMMA glass.[52] Results will be shown for a single value of $\psi^{-1} = k_B T/\sigma^3$ in eq 10; calculations that illustrate the effect of this numerical prefactor are given in the Appendix.

Most calculations are performed under the "quench-and-wait" protocol, illustrated in Figure 1. This corresponds to preparing samples by very rapid quenching to a temperature below T_g, followed by waiting a fixed (but variable) amount of time before performing the mechanical measurement. Here the control parameters are quench temperature, preaging or waiting time, and strain rate. However, many experiments in the literature use various more complex thermal history protocols. To crudely mimic one of these, we will explore to a limited extent an "anneal-and-quench" protocol, as also illustrated in Figure 1. The primary consequence of this protocol is on the temperature dependence of subtle features of the stress−strain response, mainly the strain softening amplitude (SSA), i.e., the height of the stress overshoot. We emphasize that in real experiments an unambiguous extraction of the SSA is generally not possible due to overlap of the strain softening and strain hardening responses and hence the lack of a well-defined "plateau flow stress".

III. YIELDING AND STRAIN SOFTENING

A. Stress−Strain Response and Effect of Deformation on Density Fluctuations and Segmental Relaxation. Figures 2, 3, and 4 show representative calculations for the evolution of stress, density fluctuation amplitude, and segmental relaxation time as a function of strain for varying preaging times ($T = T_g - 30$ K, $\dot{\gamma} = 0.001$ s^{-1}), strain rates ($T = T_g - 30$ K, $t_{age} = 10^5$ s), and temperatures ($t_{age} = 10^5$ s, $\dot{\gamma} = 0.001$ s^{-1}), respectively, under the "quench-and-wait" protocol. In general, one sees that the stress initially rises rapidly and reaches a maximum that defines the experimental yield stress and strain, then decreases, and gradually approaches the plastic flow plateau. Consistent with experimentally based conclusions of McKenna,[2] the thermodynamic or structural state (here quantified by S_0) is very nearly unperturbed by stress in the preyield regime (Figures 2−4b), despite the fact that the mean relaxation time is dramatically reduced (Figures 2−4c). This implies the dominant origin of the acceleration of segmental relaxation under constant deformation rate conditions is landscape tilting. The strain softening or stress-drop feature is closely correlated with the rejuvenation process (increase of S_0) as manifested by the facts: (i) the softening emerges immediately after the onset of an upturn of

S_0, (ii) the softening process and increase of S_0 expand in breadth to the same extent, and (iii) strain softening is absent for freshly quenched glass (t_{age} = 0 curve in Figure 2a) for which aging dominates over rejuvenation (no rise of S_0). Hence, we propose the origin of the strain softening and stress overshoot phenomena is mechanical enhancement of density fluctuations. The mean relaxation time is very weakly perturbed by softening, with only a small kink feature around the yield strain and/or a small gradual shift of the onset of the flow plateau being evident. This weak response originates from the two opposing contributions: (i) a stress drop slows down relaxation (landscape tilting effect), and (ii) an increase of S_0 accelerates relaxation.

We now identify specific trends in Figures 2−4. As previously discussed,[31] the plastic flow state is a function of cooling depth and strain rate (in a constant strain rate experiment) but is rigorously independent of preaging time and thermal history since it reflects the balance between aging and deformation-induced disordering as does the nonequilibrium steady state in creep. Figure 2 shows the preaging time dependence of stress, S_0, and relaxation time as a function of strain at fixed $T = T_g - 30$ K and $\dot{\gamma} = 0.001$ s^{-1}. All curves converge to the same plateau, reflecting an identical plastic flow state ("erasure of thermal history"); the amplitude of the overshoot (SSA) in stress−strain curves grows monotonically with initial waiting time. These results are consistent with experiment.[28] One sees from Figure 2a the yield strains are of order 5%, and a strain of ∼20−30% is required to achieve the plastic flow stress plateau. The latter is comparable to the strain typically observed in polymer glasses for the onset of strain hardening (upswing of stress).[3−5] Figure 2b shows that the density fluctuation amplitude monotonically decreases with strain under quenched conditions (no preaging, but small aging during the mechanical test), compared to the preaged samples where the density fluctuation amplitude grows with strain. Importantly, note the relatively small changes of the structural order parameter, 4% or less, which nevertheless have large mechanical consequences. Figure 2c shows the quiescent relaxation times vary from 10^4 to 10^7 s depending on preaging protocol, but in the plastic flow regime they all decrease enormously to ∼30 s. By the standard kinetic vitrification criterion, one can say deformation has induced a "glass-to-liquid" transition.

Calculations of strain-rate-dependent response at fixed temperature $T = T_g - 30$ K and preaging time $t_{age} = 10^5$ s are shown in Figure 3. Higher strain rate implies stronger rejuvenation (eq 9) which pushes the system up the landscape to a more disordered state (large S_0 plateau in Figure 3b) and also leads to an increase of the "onset" strain. The stress−strain curves saturate at different stresses at large strains mainly as a consequence of the strain-rate-dependent "yield/flow criterion" of eq 17[14,15] and also the distinct values of S_0. The SSA increases with strain rate, reflecting the fact that although the yield and flow stresses both grow roughly logarithmically with deformation rate, the prefactors are different. One deduces the yield peak is more sensitive to strain rate, an understandable consequence of it being influenced by rejuvenation effects in contrast to the flow stress. The evolution with strain of the density fluctuation amplitude is complex in the sense that different strain rate curves cross, reflecting a difference in the dependence of onset strain and limiting plateau value on strain rate.

Extra complexity arises when temperature is varied because both the initial aged state and steady flow state depend on temperature. Figure 4 shows calculations at temperatures that vary from 10 to 60 K below T_g at a fixed $t_{age} = 10^5$ s and $\dot{\gamma} = 0.001$ s^{-1}, corresponding to the "quench-and-wait" protocol. The yield stress, flow stress, and yield strain all grow upon cooling, and the flow plateau emerges at strains ∼30−40% (Figure 4a). Here, the quenched S_0 is a monotonic decreasing function of cooling depth, but the aging dynamics slows down as well which leads to the nonmonotonic initial S_0 in Figure 4b. In contrast, the steady state value of S_0 is a monotonic decreasing function of cooling depth at fixed strain rate. Figure 4c again shows remarkably large decreases of the relaxation time due to deformation, to absolute values below the typically smallest value used to define a glass of 100 s. Close inspection of Figure 4a reveals the stress overshoot or SSA varies nonmonotonically with temperature and is positively correlated with the difference of $S_{0,pf} - S_{0,i}$, where $S_{0,pf}$ is the density fluctuation amplitude under steady state plastic flow conditions and $S_{0,i}$ the initial density fluctuation amplitude.

B. Strain Softening Amplitude. As established in Figures 2−4, strain softening is closely correlated to the initial age state and final flow state and reflects a competition between aging and mechanical rejuvenation. We now systematically investigate the preaging time, strain rate, and temperature dependences of the SSA. Note the latter is uniquely defined in our present theory (that ignores hardening) as the difference of the yield and plastic flow stresses, $\Delta\tau_{os}$.

Figure 5a shows the SSA and its nondimensionalized analogue (nSSA) reduced by corresponding plastic flow stress ($\Delta\tau_{os}/\tau_{pf}$), as a function of logarithmic preaging time for five strain rates and fixed $T = T_g - 30$ K. The curves start from zero and, after a threshold preaging time, rapidly cross over to a roughly logarithmic growth. The existence of a threshold and subsequent logarithmic growth has been observed in the experiments of Klompen et al.[53] The logarithmic growth follows directly from the fact that both the yield and flow stresses age logarithmically with waiting time, albeit with different numerical prefactors. Note that this threshold shifts to shorter waiting time (i.e., stronger aging dynamics) at higher strain rates (i.e., stronger rejuvenation), and the solid curves in Figures 2−4 show that strain softening is absent (present) when aging (rejuvenation) dominates. These results suggest that the threshold represents a critical balance point between aging and rejuvenation. All solid S_0 curves in Figures 2−4 are monotonic functions of deformation; i.e., either aging (when $S_{0,i} > S_{0,pf}$) or rejuvenation (when $S_{0,i} > S_{0,pf}$) dominates during the entire deformation. To avoid any confusion, we emphasize that aging and rejuvenation are concomitant processes present during the entire deformation (see eq 10). Figures 2−4 show that, in most cases, the practical dominance of one of these processes over the other during the whole deformation implies either S_0 monotonically increases ($S_{0,i} < S_{0,pf}$), or monotonically decreases ($S_{0,i} > S_{0,pf}$), even though both processes are present.

Given the above, in order to further understand the critical crossover from the regime of aging dominance to rejuvenation dominance, we calculate $S_{0,i} = S_{0,pf}$ at fixed $T = T_g - 30$ K and $\dot{\gamma} = 0.000\,01$ s^{-1} (dashed curves in Figure 3). We find that aging and rejuvenation do not balance over the whole deformation; instead, aging dominates in the beginning, and then rejuvenation takes over (Figure 3b), resulting in a shallow minimum, $S_{0,min}$, at intermediate strain. This weak unbalance results in a small SSA of 0.84 MPa in Figure 3a and again implies that a rejuvenation dominated process during deformation is the origin of strain softening. The critical crossover occurs at a certain $S_{0,i} > S_{0,pf}$, above which $S_{0,pf} = S_{0,min}$; i.e., aging dominates over the whole deformation range. The increase of SSA with preaging time in Figure 5a should, in principle, terminate around the long "equilibration" time for reaching the fully aged state which is unreachable at low temperature in a practical experiment.

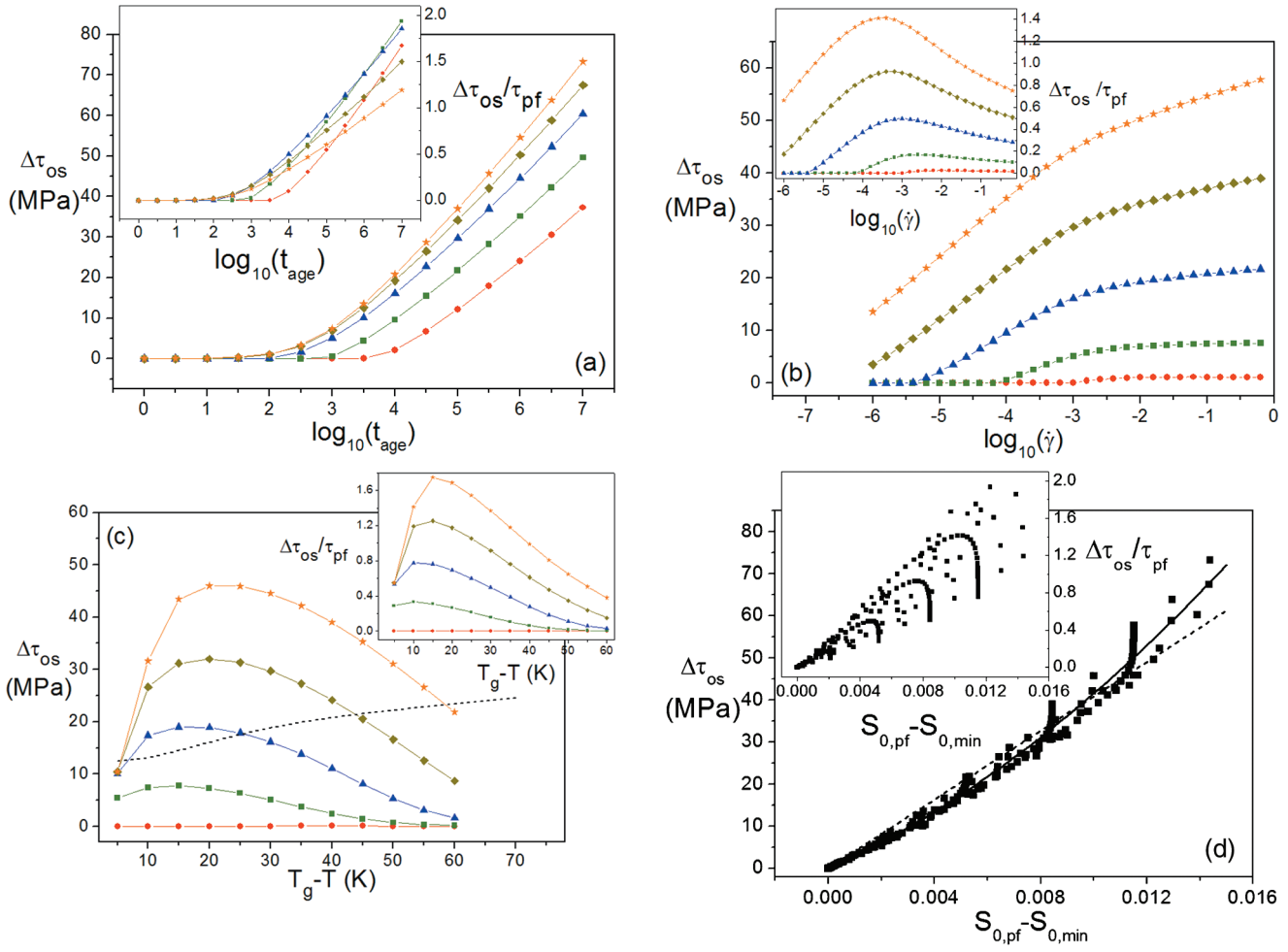

Figure 5. Strain softening amplitude in MPa, $\Delta\tau_{os}$, as a function of (a) logarithmic preaging time (in seconds) at fixed $T = T_g - 30$ K and strain rates $\dot{\gamma} = 10^{-5}$, 10^{-4}, 10^{-3}, 10^{-2}, and 10^{-1} s^{-1} from bottom to top; (b) logarithmic strain rates at fixed $T = T_g - 30$ K and for preaging times $t_{age} = 10^2$, 10^3, 10^4, 10^5, and 10^6 s from bottom to top; (c) cooling depth at fixed strain rate $\dot{\gamma} = 10^{-3}$ s^{-1} and for preaging times $t_{age} = 10^2$, 10^3, 10^4, 10^5, and 10^6 s from bottom to top, where the dashed curve shows the calculation based on "anneal-and-quench" protocol with an annealing temperature of $T_g - 5$ K. (d) Scatter plot of $\Delta\tau_{os}$ versus the difference between the steady state value and the minimum value of the dimensionless density fluctuation amplitude for all data points in (a), (b), and (c); dashed and solid curves are linear and second-order polynomial fits, respectively. Insets show the corresponding nondimensionalized SSA reduced by plastic flow stress.

An analogous threshold appears in the strain-rate dependence of the SSA for five preaging times and fixed temperature of $T = T_g - 30$ K (Figure 5b). Beyond the threshold strain rate, the curves exhibit two regimes: (i) roughly logarithmic growth at small strain rate and (ii) crossover at a strain rate of $\sim 10^{-3}$–10^{-2} s^{-1} to a slower increase which approaches a long time saturated maximum value characterizing a fully rejuvenated state in the high strain rate limit. The increase of strain softening with deformation rate is generically observed in experiment.[30] The calculated nSSA is nonmonotonic and shows a peak at moderate strain rate, revealing a transition from relatively stronger to weaker rate dependence of SSA as compared to the plastic flow stress. The nonmonotonic behavior can be understood to be a consequence of the SSA, but not the flow stress, saturating at high strain rates, thereby resulting in a decrease of the nSSA amplitude at high rates; on the other hand, at low strain rates there is a threshold for the emergence of the SSA (from zero) but not flow stress, and hence the nSSA increases with rate.

Figure 5c presents calculations of the SSA as a function of cooling depth. A nonmonotonic variation is predicted for the "quench-and-wait" protocol, which can be understood primarily as a consequence of two competing factors: (i) faster aging at higher temperature and (ii) $S_{0,l}$ and $S_{0,g}$ are closer at higher T. Specifically, considering high strain rate conditions (strong rejuvenation, $S_{0,pf} \sim S_{0,g}$), Figure 5d shows the SSA is positively correlated with the variation of density fluctuation amplitude $S_{0,f} - S_{0,min} \sim S_{0,g} - S_{0,min}$, or mostly $S_{0,g} - S_{0,i}$. At high temperature close to T_g, the glass is fully aged, i.e., $S_{0,g} - S_{0,i} \sim S_{0,g} - S_{0,l}$ which increases with cooling. However, at low temperature the glass is not fully aged, and hence $S_{0,g} - S_{0,i}$ decreases with cooling since aging is much slower. Therefore, the SSA grows with cooling for temperatures close to the glass transition and decreases at low temperature. Moreover, when the preaging time increases, the glass can be fully aged even at lower temperature which results in a shift of the peak to lower temperatures as seen in Figure 5c; of course, other factors can affect the quantitative location of the SSA maximum.

The predicted nonmonotonic variation of the SSA would seem to contradict some experimental observations that the overshoot either saturates at low temperature or continues to grow.[26,54−57] We believe this is a subtle issue due to the high sensitivity of the thermal behavior of the SSA to initial state. Our

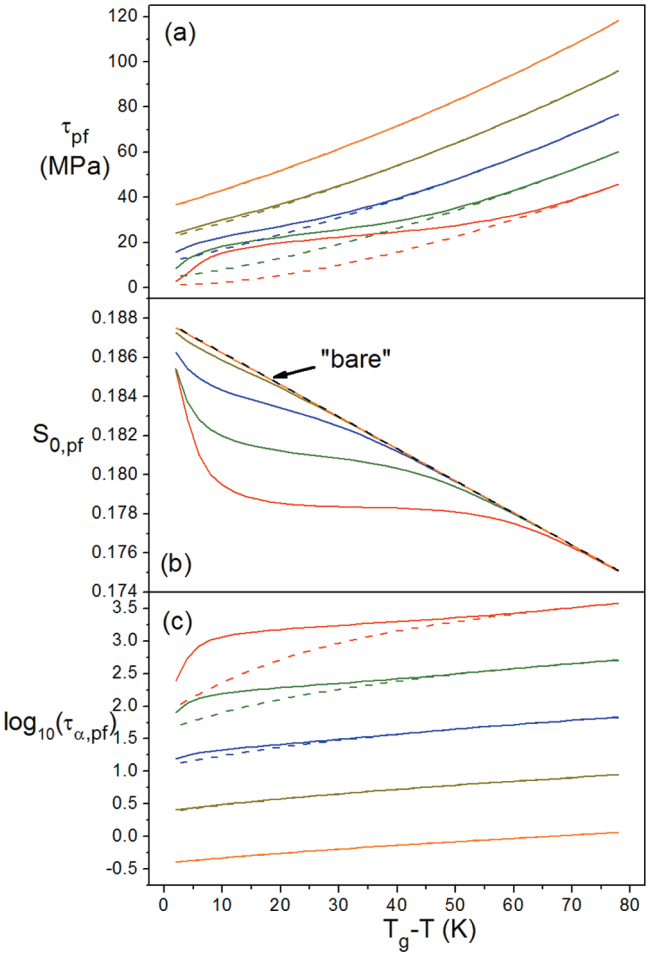

Figure 6. Steady state (a) flow stress, (b) dimensionless density fluctuation amplitude, and (c) logarithmic mean relaxation time (in seconds), as a function of degree of undercooling for strain rates $\dot{\gamma} = 10^{-5}$, 10^{-4}, 10^{-3}, 10^{-2}, and 10^{-1} s^{-1} from bottom to top in (a) and (b) and from top to bottom in (c). Dashed curves are analogous calculations based on the "bare" constitutive equation relevant for quenched glasses in the absence of aging and rejuvenation.[15]

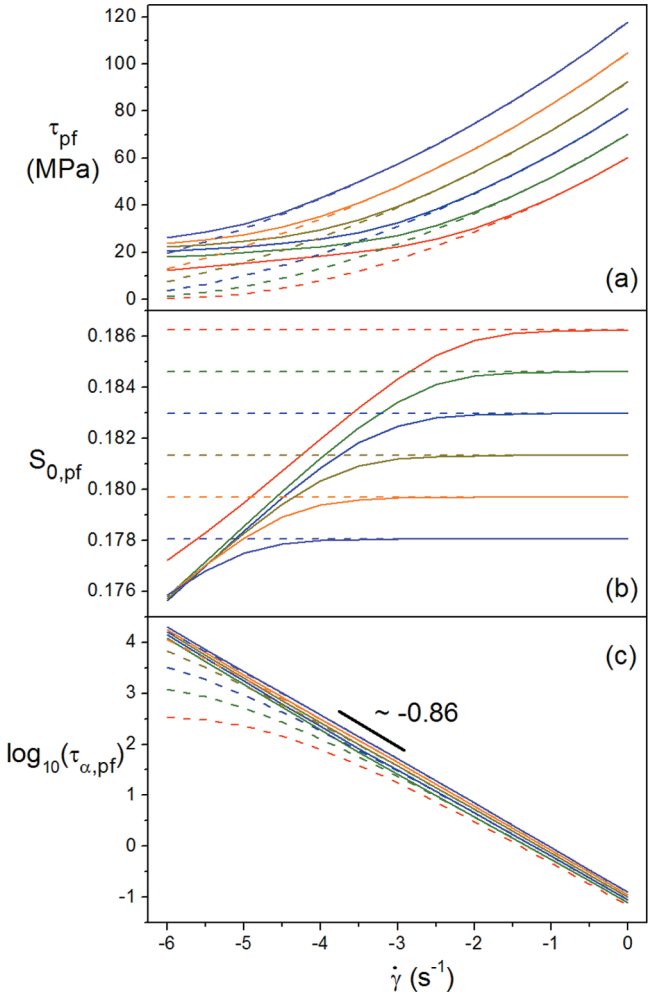

Figure 7. Strain-rate dependence of same quantities as in Figure 6 for cooling depths $T = T_g - 10$ K, $T_g - 20$ K, $T_g - 30$ K, $T_g - 40$ K, $T_g - 50$ K, and $T_g - 60$ K from bottom to top in (a) and (c) and from top to bottom in (b). Dashed curves are analogous calculations based on the "bare" constitutive equation under quenched conditions.[15]

prediction is based on the "quench-and-wait" protocol. However, for many samples as-received, upon annealing or more complex heat treatment there are complications associated with the finite rate of cooling, identification of T_g, etc. Also, there does exist experimental data that supports the nonmonotonic behavior.[25,58] For example, measurements on semiaromatic polyamides[27] have shown a peak close to T_g (sub-T_g regime) in the SSA—temperature plot, although the data are noisy.

To demonstrate the sensitivity of strain softening on the thermal history prior to the mechanical measurement, we have performed additional calculations based on "anneal-and-quench" protocol, i.e., first fully anneal the sample at a certain temperature slightly *below* T_g then rapidly quench it to the test temperature. We now obtain a SSA that does monotonically increase upon cooling for the shown case where the annealing temperature is $T_g - 5$ K (dashed curve in the main panel of Figure 5c). We emphasize that the issue of complex heat treatment and other experimental protocol aspects affecting a qualitative trend is only relevant for the thermal dependence of subtle quantities such as the SSA which is the difference of two large numbers (yield peak and flow stress). Moreover, experimental SSA data usually have intrinsic ambiguity due to the overlap of the strain softening and hardening responses (which do not have the same temperature dependences) and hence exhibit an absence of a plateau flow stress.

On the basis of our analysis, strain softening is closely connected to the rejuvenation process during deformation. The underlying physics is that the increase of the density fluctuation amplitude due to mechanically generated disorder (rejuvenation) diminishes the elastic modulus and speeds up relaxation beyond the effect of landscape tilting mechanism. The softening amplitude apparently depends positively on the amount of rejuvenation as quantified by the change of the density fluctuation amplitude, $\Delta S \equiv S_{0,pf} - S_{0,min}$, which is zero above the critical crossover. Far below the crossover, $\Delta S \approx S_{0,pf} - S_{0,i}$; i.e., rejuvenation dominates over the entire deformation. A scatter plot of the SSA as a function of the amount of rejuvenation is shown in Figure 5d based on the calculations in Figure 5a—c. The data distribute narrowly in a roughly linear regime which can be fit by $\Delta\tau_{os} = 4088\Delta S$ (dashed line) or even better as $\Delta\tau_{os} = 2850\Delta S + 130548\Delta S^2$ (solid curve). On the contrary, the nSSA results (inset) distribute widely forming a "slice-of-pizza" area.

dx.doi.org/10.1021/ma200436w |*Macromolecules* 2011, 44, 3988–4000

IV. NONEQUILIBRIUM STEADY PLASTIC FLOW AND COMPARISON WITH EXPERIMENT AND SIMULATION

A. Plastic Flow. Steady state plastic flow in a constant strain rate response is the analogue of the nonequilibrium steady state in the creep (constant stress) investigated in ref 31. As demonstrated in Figure 2, thermal history is erased, and the flow state is only a function of temperature and strain rate. Figure 6 shows the temperature dependences of the steady state flow stress, density fluctuation amplitude, and logarithmic relaxation time for five strain rates. Analogous calculations based on the same constitutive equation but in the absence of aging and mechanical disordering (i.e., for quenched or fully rejuvenated glasses)[15] are shown for comparison (dashed curves); we have previously demonstrated our theory predicts very well the stress−strain response under quenched conditions.[15] At high strain rate (strong mechanical disordering) or low temperature (weak aging dynamics), the nonequilibrium steady state is nearly "fully rejuvenated" (i.e., S_0 is almost the freshly quenched value), leading to overlap of the two types of calculations for all three properties. However, clear differences are seen at high temperature and low strain rate. A weak upturn (downturn) thus appears in the flow stress and logarithmic relaxation time (density fluctuation amplitude) curves at low strain rate at ∼5−10 K below T_g. Some flow stress data in the literature seems to support such trends,[25,26] although accurate measurements are difficult. Other general features are that the density fluctuation amplitude in the plastic flow regime (Figure 6b) monotonically decreases as temperature is lowered, and the steady state alpha relaxation time is very weakly dependent on temperature but strongly deformation rate dependent.

The strain-rate dependence of the three quantities studied in Figure 6 are shown in Figure 7. There appears to be two regimes of plastic flow response. Under quenched conditions, the dependence is almost simple logarithmic. In the low strain rate limit, the density fluctuation amplitude approaches the fully aged value (Figure 7b), which is the origin of the upturn of the plastic flow stress at low strain rate (Figure 7a). The steady state amplitude of density fluctuations is clearly more strain rate sensitive as the glass becomes colder.

Figure 7c presents results for the steady state alpha relaxation time in the format commonly adopted to describe "shear thinning" of complex fluids. The dashed curves show the corresponding results for a quenched glass,[15] and one sees a crossover to a plateau at low strain rate representing quiescent relaxation. But no such crossover is observed in the strain rate window of Figure 7 when physical aging and mechanical rejuvenation (solid curves) are operative; such a crossover can only appear at much lower strain rates corresponding to the inverse of the quiescent (now much smaller) relaxation time of the fully aged material. Note that at high strain rates both the slopes and absolute value of relaxation times of all systems (quenched or not quenched) are remarkably similar. Moreover, in this regime the relaxation time is liquidlike, i.e., <100 s. The form of the dependence is an inverse power law with a shear thinning exponent of ∼−0.86. This behavior agrees with recent experiments[7] and simulations[12,59] under creep deformation. Moreover, it is very similar to experiments on highly sheared colloidal glasses,[60] the behavior of which is well predicted by the nonlinear rheology version of NLE theory.[61] Although we have not been able to derive an analytic expression for the apparent shear thinning exponent, what controls its (weakly) nonuniversal magnitude is clear from prior colloid and polymer studies based on the NLE approach. Specifically, as the quiescent relaxation time of a system

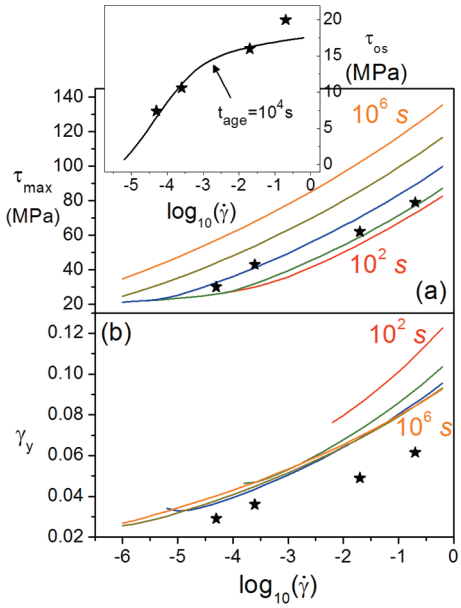

Figure 8. (a) Yield stress and (b) yield strain as a function of logarithmic strain rate for $\Delta T = T_g - T = 35$ K and preaging times $t_{age} = 10^2$, 10^3, 10^4, 10^5, and 10^6 s. Experimental PMMA data extracted from ref 25 are shown as asterisks. The inset of (a) shows the corresponding SSA.

increases (cooling in the polymer glass or increasing volume fraction for colloidal suspensions), the absolute value of the apparent thinning exponent gently increases (stronger thinning). This occurs since the absolute yield stress (defined as when the activation barrier goes to zero) is a rather weak function of temperature,[15] or volume fraction,[61] and hence the drop of the relaxation time with stress becomes more dramatic if the quiescent state dynamics is slower.

B. Yield Stress, Strain, and Overshoot: Comparison with Experiment and Simulation. We now compare our theoretical calculations with measurements by Tordjeman et al.[25] The yield stress and strain defined at the "yield peak" depend on thermal history, cooling depth, and deformation rate. The initial age states of their PMMA samples[25] prior to mechanical measurement are unclear, which prevents a precise quantitative comparison. Additional potentially complicating factors of varying degree of importance are (i) two kinds of PMMA samples were studied with different glass transition temperatures (392 and 399 K) while $T_g = 378$ K in our theory; (ii) the statistical segment length, σ, is not uniquely definable and enters the computation of the absolute magnitude of stress via the factor k_BT/σ^3; and (iii) the a priori unknown numerical prefactor ψ in eq 10 quantitatively modifies the ratio of contributions from aging and rejuvenation. Therefore, the comparisons below only aim to establish the reasonability of the theoretical predictions. We continue to use the same set of PMMA material parameters as mentioned in the beginning of section III and do not vary them to fit experimental data. Comparisons of theory and experiment are made based on matching the degree of cooling, $\Delta T = T_g - T$.

Figures 8 and 9 (solid curves) show the logarithmic strain-rate and cooling-depth dependences, respectively, of the yield stress and strain for preaging times from 10^2 to 10^6 s, corresponding to a "quench-and-wait" protocol. Experimental PMMA glass data extracted from Figure 7 of ref 25 are presented as asterisks. In Figures 8a and 8b, one

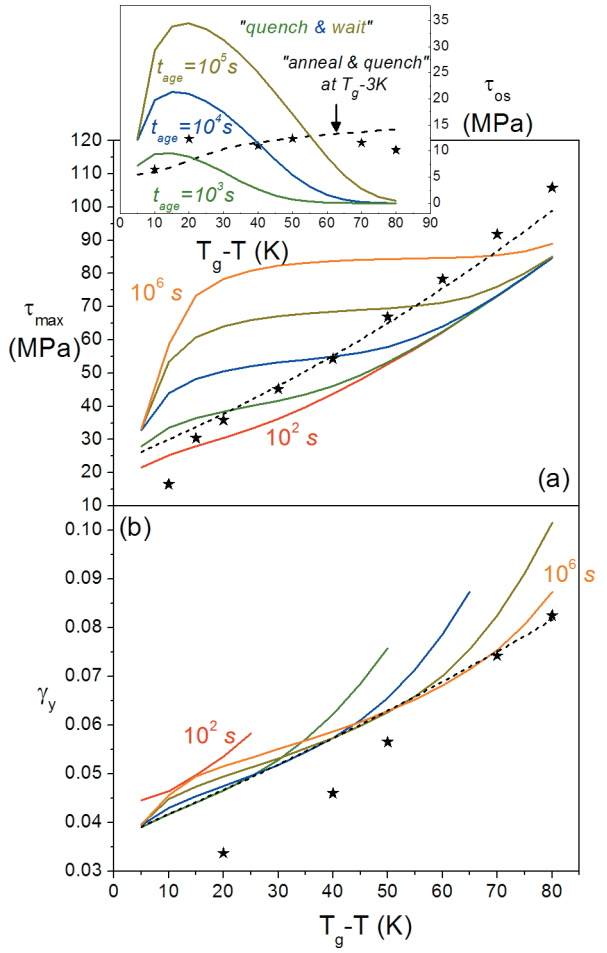

Figure 9. Cooling depth dependence of same quantities as in Figure 8 for a strain rate $\dot{\gamma} = 2 \times 10^{-3}$ s^{-1} and preaging times $t_{age} = 10^2$, 10^3, 10^4, 10^5, and 10^6 s (solid curves). Dashed curves show results based on "anneal-and-quench" protocol at an annealing temperature $T = T_g - 3$ K. Asterisks are experimental PMMA data.[25] The inset of (a) shows the corresponding SSA.

sees the theoretical yield stress and strain grow roughly logarithmically, but weakly upwardly curved, with strain rate. The experimental yield stresses are distributed between the curves for preaging times of 10^3 and 10^4 s, perhaps suggesting the experimental samples experienced a similar thermal history. The inset shows the stress overshoot amplitude at a fixed preaging time that is appropriate for achieving reasonable agreement with the yield stress. Rather good agreement can be seen. Figure 8b presents the corresponding yield strains, which are in reasonable accord with experiment but systematically too high.

The thermal dependence of the theoretical yield stresses in Figure 9a covers most of the experimental yield stresses observed at different cooling depths, but the experimental data distribute widely among the curves. This suggests our calculation based on a "quench-and-wait" protocol may not be suitable. Hence, we have also performed computations based on the "anneal-and-quench" protocol at an annealing temperature of $T_g - 3$ K, shown as dashed curves in Figure 9a. The agreement of theory and experiment for the yield stress is satisfying. As found in Figure 8b, the theoretical yield strains in Figure 9b are larger than experiment, for both protocols. The inset in Figure 9 shows the SSA for both "quench-and-wait" and "anneal-and-quench" protocols. The former predicts a nonmonotonic variation with cooling, while the latter predicts a thermal dependence in reasonable agreement with experiment. We conclude the thermal dependences of the yield stress, yield strain, and stress overshoot are quite well captured by the theory based on the "anneal-and-quench" protocol.

Finally, we make a few brief remarks concerning the relationship of our results with simulations of Rottler and Robbins,[62] who investigated the combined effect of aging and strain rate in a quench-and-wait protocol on the yield stress of a simple Lennard-Jones glass. In agreement with our calculations (main panel of Figure 8a), the simulations find the yield stress depends logarithmically on strain rate and aging time. Two different regimes of rate sensitivity were found depending on the time it takes to strain to yield. Moreover, their data for different rates and aging times could be collapsed on to a master curve. In agreement with these simulations, our calculations in Figure 8 also show two different regimes of rate sensitivity for aging times of 10^2, 10^3, and 10^4 s. If we replot our calculations based on the scheme of Rottler and Robbins,[62] we find the theoretical yield stress results do collapse on to a master curve for long waiting time (10^4, 10^5, and 10^6 s) if small vertical shifts are employed (not shown); the 100 s waiting time calculations can also be collapsed but only if an additional horizontal shift is applied. Our predicted crossover between the two rate sensitivity regimes occurs at $\dot{\gamma} t_{age} \approx 0.03-0.1$. Interestingly, the threshold for the emergence of strain softening in Figures 5a and 5b occurs at not too dissimilar values of $\dot{\gamma} t_{age} \approx 0.03-3$, which suggests their probable correlation.

V. SUMMARY

We have applied the recently extended nonlinear Langevin equation theory of segmental relaxation, elasticity, and nonlinear mechanical response of deformed polymer glasses with physical aging and mechanical rejuvenation to study yielding, strain softening, and plastic flow under a constant strain rate deformation. The density fluctuation amplitude is the key structural variable that quantifies the segmental transient localization and relaxation processes in the glass. Detailed calculations of stress−strain response, density fluctuation amplitude, and segmental alpha relaxation time during deformation, and their strain rate, temperature, and preaging time (thermal history) dependences, have been presented for parameters that model PMMA glass.

We find deformation does not significantly alter the structural order parameter under preyield conditions, but the relaxation time is dramatically reduced with increasing strain and stress due to the landscape tilting mechanism. In the postyield regime beyond the yield peak, the softening and rejuvenation processes are positively correlated with regards to their influence on the amplitude and strain range of the stress overshoot feature. Detailed calculations reveal the softening behavior does not depend directly on the difference between initial and steady plastic flow states, but rather on whether there exists a rejuvenation-dominated process during deformation and the corresponding rejuvenation amplitude. The thresholds of preaging time and strain rate beyond which the softening behavior emerges determine when the rejuvenation process becomes important. Quantitatively, the amplitude of the stress overshoot (SSA) is roughly proportional to the rejuvenation amplitude as quantified by $S_{0,pf} - S_{0,min}$. Predictions for the preaging time and strain rate dependences of the SSA are consistent with experiment. However, the temperature dependence of the SSA is nonmonotonic

under the "quench-and-wait" protocol versus the monotonic growth with cooling that can be realized under the "anneal-and-quench" protocol. Calculations based on the latter seem consistent with PMMA glass experiments. More generally, the issue of experimental protocol is not very important except for the subtle (and relatively low) SSA amplitude as a function of temperature.

Calculations of the temperature and strain rate dependences of the plastic flow stress, density fluctuation amplitude, and relaxation time in the long time (large strain) nonequilibrium steady state were performed both in the presence and absence of physical aging and mechanical rejuvenation. Deviations between these two situations are evident at low strain rates and high temperatures but tend to disappear when approaching T_g. Despite the uncertainties of the initial state of experimental samples, the theory gives reasonable predictions for the rate and cooling-depth dependences of yield (peak) stress and yield strains. We also investigated the role of the numerical prefactor ψ that enters the disorder production rate in eq 10 (see Appendix). Both the yield and steady state values vary only slightly even when this parameter is changed by 2 orders of magnitude, and none of the predicted temperature, rate, and preaging-time dependences qualitatively change.

In the present work, polymer chain deformation and the associated strain hardening effect observed in most thermoplastics at large deformations have been ignored. We have formulated and applied a theory for hardening in the absence of physical aging and mechanical rejuvenation, as relevant to quenched glasses.[23] However, integrating the hardening process with aging and rejuvenation effects is a nontrivial open problem which requires careful future study.

In order to better test the breadth of applicability of the theoretical ideas (especially S_0 as the key structural variable) underlying our approach, future work is required to quantitatively address specific experimental studies on glasses such as PMMA, polystyrene, and polycarbonate.[3,19−21] More complex protocols are also of interest. For example, one can ask to what extent will the deformed-and-unloaded glass be different from the original well-aged material. Our present theory is able to predict the mechanical response under an anneal−deform−unload protocol if the deformation does not enter the strain hardening regime. The evolution of S_0 can be computed, and after such a mechanical test a well-aged sample is rejuvenated to a degree that increases with load. One can also ask to what extent thermal rejuvenation differs from its mechanical analogue. Since there is no consensus definition of the "end point" of the mechanical rejuvenation process, we have made a minimalist assumption (per Langer[49]) of not distinguishing between thermally (freshly quenched) and fully mechanically rejuvenated states. However, as we cautioned in our prior recent work,[31] the freshly quenched state is not unique since it depends on cooling rate (a presumably minor effect), and the mechanically fully rejuvenated state may correspond to a system at an effective temperature (or degree of disorder) above T_g, perhaps as high as the mode coupling crossover or dynamical onset temperature.

Finally, as a general comment, we remind the reader that the present work has employed the minimalist analytic version of polymer NLE theory. Since its focus is on the mean relaxation time and mechanical properties within a homogeneous material framework, spatial and temporal dynamic heterogeneity (DH) effects, such as a relaxation time distribution, are not taken into account. This must imply some limitations of the approach. However, since our analytic polymer NLE theory has had many successes in describing the nonlinear relaxation and mechanical responses of glasses,[37,38] DH effects may be of secondary importance, at least for some questions. But, this issue certainly needs much further careful study, and understanding phenomena such as stretched exponential relaxation and its dependence on applied stress must go beyond a dynamical mean-field approach. In this context, it is important to emphasize that numerical implementation of the full stochastic NLE theory via trajectory simulation does include a host of DH effects as extensively demonstrated in the context of glassy colloid suspensions[63] and the analytic extension to treat a static distribution of activation barriers.[64]

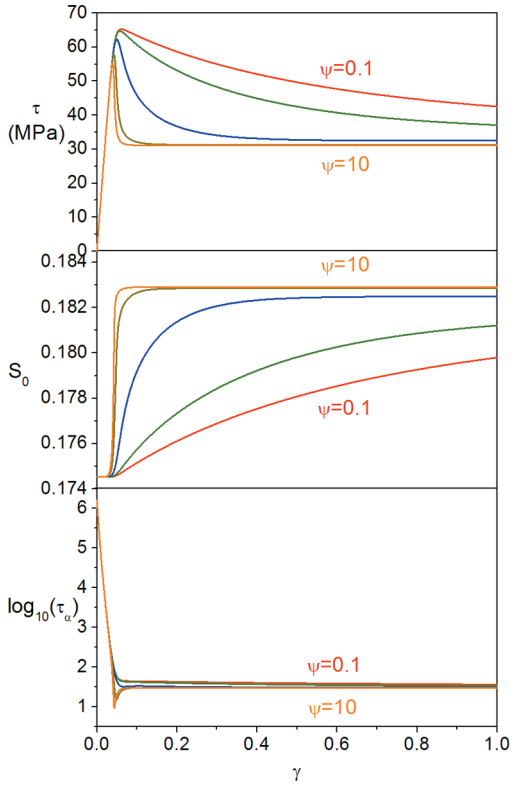

Figure 10. Results analogous to those in Figure 2 for $T = T_g - 30$ K, $\dot{\gamma} = 10^{-3}$ s^{-1}, and $t_{age} = 10^5$ s but with varied numerical prefactor in eq 10; $\psi = 0.1$, 0.2, 1, 5, and 10 from top to bottom in (a) and (c) and bottom to top in (b).

APPENDIX. INFLUENCE OF THE PREFACTOR IN THE REJUVENATION TERM

We have carefully investigated the role of the a priori unknown numerical prefactor, ψ, in eq 10 which controls the ratio of contributions from physical aging and mechanical disordering and thus influences quantitative aspects of yielding, softening, and the steady state value of density fluctuation amplitude, $S_{0,pf}$. The prefactor was set to unity in all calculations reported in the main text. We have performed many additional calculations over a wide range of ψ values for various strain rates, temperatures, and preaging times. Figure 10 shows one representative example for $T = T_g - 30$ K, $\dot{\gamma} = 10^{-3}$ s^{-1}, and $t_{age} = 10^5$ s. One sees the following trends as ψ (in units of σ^3/k_BT) increases by 2 orders of magnitude from 0.1 to 10: (i) the yield stress decreases by 15%, (ii) the yield strain decreases by 34%, (iii) the alpha relaxation time behavior changes significantly only around the shallow peak

region by at most 1 order of magnitude, and (iv) the quantitative aspects of the softening and rejuvenation processes change dramatically as expected; i.e., the evolution with strain becomes sharper and narrower upon increasing ψ. For small ψ, the softening process extends to very large strain beyond the onset of hardening in experiments. Theoretically, we find the steady state value $S_{0,\infty}$ or $S_{0,pf}$ increases only by 0.9%, while the flow stress increases by 16% when ψ increases from 0.1 to 10. Despite the modest quantitative changes that occur when ψ is varied, all calculations of the yield stress, yield strain, and SSA show the same qualitative dependences on temperature, strain rate, and preaging time.

AUTHOR INFORMATION

Corresponding Author

*E-mail: kangchen@suda.edu.cn (K.C.), kschweiz@illinois.edu (K.S.S).

ACKNOWLEDGMENT

The early stages of this work were performed at Illinois and funded by NSF-NIRT Project No. 0505840. Present support is from the DOE-BES Materials Science and Engineering via Oak Ridge National Lab (K.S.S.) and the National Natural Science Foundation of China under Grant No. 11074180 (K.C.). We are very grateful to Leon Govaert for discussions, correspondence, and sending us helpful literature references concerning polymer glass mechanics. We also thank Mark Ediger and James Langer for discussions of the competition between physical aging and mechanical rejuvenation.

REFERENCES

(1) Angell, C. A.; Ngai, K. L.; McKenna, G. B.; McMillan, P. F.; Martin, S. W. *J. Appl. Phys.* **2000**, *88*, 3113–3157.
(2) McKenna, G. B. *J. Phys.: Condens. Matter* **2003**, *15*, S737–S763.
(3) Meijer, H. E. H.; Govaert, L. E. *Prog. Polym. Sci.* **2005**, *30*, 915–938.
(4) Haward, R. N.; Young, R. J. *The Physics of Glassy Polymers*; Chapman and Hall: London, 1997.
(5) Ward, I. M.; Hadley, D. W. *Introduction to Mechanical Properties of Solid Polymers*; Wiley and Sons: New York, 1993.
(6) Rubinstein, M.; Colby, R. H. *Polymer Physics*; Oxford University Press: Oxford, 2003.
(7) Lee, H. N.; Paeng, K.; Swallen, S. F.; Ediger, M. D. *Science* **2009**, *323*, 231–234.
(8) Lee, H. N.; Paeng, K.; Swallen, S. F.; Ediger, M. D. *J. Chem. Phys.* **2008**, *128*, 134902.
(9) Lee, H. N.; Paeng, K.; Swallen, S. F.; Ediger, M. D.; Stamm, R. A.; Caruthers, J. M. *J. Polym. Sci., Part B: Polym. Phys.* **2009**, *47*, 1713–1727.
(10) Riggleman, R. A.; Lee, H. N.; Ediger, M. D.; de Pablo, J. J. *Soft Matter* **2010**, *6*, 287–291.
(11) Lee, H. N.; Ediger, M. D. *Macromolecules* **2010**, *43*, 5863–5873. *J. Chem. Phys.* **2010**, *133*, 014901.
(12) Riggleman, R. A.; Schweizer, K. S.; de Pablo, J. J. *Macromolecules* **2008**, *41*, 4969–4977.
(13) Lyulin, A. V.; Balabaev, N. K.; Mazo, M. A.; Michels, M. A. J. *Macromolecules* **2004**, *37*, 8785–8793. Lyulin, A. V.; Vorelaars, B.; Mazo, M. A.; Michels, M. A. J. *Europhys. Lett.* **2005**, *71*, 618–624.
(14) Chen, K.; Schweizer, K. S. *Europhys. Lett.* **2007**, *79*, 26006.
(15) Chen, K.; Schweizer, K. S. *Macromolecules* **2008**, *41*, 5908–5918.
(16) Kramer, E. J. *J. Polym. Sci., Part B: Polym. Phys.* **2005**, *43*, 3369–3371.
(17) Haward, R. N.; Thackray, G. *Proc. R. Soc. London, A* **1968**, *302*, 453–472.
(18) Arruda, E. M.; Boyce, M. C. *Int. J. Plast* **1993**, *9*, 697–720. Dupaix, R. B.; Boyce, M. C. *Polymer* **2005**, *46*, 4827–4838.
(19) van Melick, H. G. H.; Govaert, L. E.; Meijer, H. E. H. *Polymer* **2003**, *44*, 2493–2502.
(20) Kierkels, J. Ph.D. Thesis, Technical University of Eindhoven, Eindhoven, The Netherlands, 2006.
(21) Govaert, L. E.; Tervoort, T. A. *J. Polym. Sci., Part B: Polym. Phys.* **2004**, *42*, 2041–2049.
(22) Wendlandt, M.; Tervoort, T. A.; Suter, U. W. *Polymer* **2005**, *46*, 11786–11797.
(23) Chen, K.; Schweizer, K. S. *Phys. Rev. Lett.* **2009**, *102*, 038301.
(24) Chui, C.; Boyce, M. C. *Macromolecules* **1999**, *32*, 3795–3808.
(25) Tordjeman, P.; Teze, L.; Halary, J. L.; Monnerie, L. *Polym. Eng. Sci.* **1997**, *37*, 1621–1632.
(26) Choe, S.; Brule, B.; Bisconti, L.; Halary, J. L.; Monnerie, L. *J. Polym. Sci., Part B: Polym. Phys.* **1999**, *37*, 1131–1139.
(27) Brule, B.; Halary, J. L.; Monnerie, L. *Polymer* **2001**, *42*, 9073–9083.
(28) Hasan, O. A.; Boyce, M. C.; Li, X. S.; Berko, S. *J. Polym. Sci., Part B: Polym. Phys.* **1993**, *31*, 185–197.
(29) Govaert, L. E.; van Melick, H. G. H.; Meijer, H. E. H. *Polymer* **2001**, *42*, 1271–1274.
(30) van Melick, H. G. H.; Govaert, L. E.; Raas, B.; Nauta, W. J.; Meijer, H. E. H. *Polymer* **2003**, *44*, 1171–1179.
(31) Chen, K.; Schweizer, K. S. *Phys. Rev. E* **2010**, *82*, 041804.
(32) Munch, E.; Pelletier, J. M.; Sixou, B.; Vigier, G. *Phys. Rev. Lett.* **2006**, *97*, 207801.
(33) Chen, K.; Schweizer, K. S. *Phys. Rev. Lett.* **2007**, *98*, 167802.
(34) Chen, K.; Schweizer, K. S. *Phys. Rev. E* **2008**, *78*, 031802.
(35) Chen, K.; Schweizer, K. S. *J. Chem. Phys.* **2007**, *126*, 014904.
(36) Chen, K.; Schweizer, K. S.; Stamm, R.; Lee, E.; Caruthers, J. M. *J. Chem. Phys.* **2008**, *129*, 184904.
(37) Chen, K.; Saltzman, E. J.; Schweizer, K. S. *J. Phys.: Condens. Matter* **2009**, *21*, 503101.
(38) Chen, K.; Saltzman, E. J.; Schweizer, K. S. *Annu. Rev. Condens. Matter Phys.* **2010**, *1*, 277–300.
(39) Schweizer, K. S. *J. Chem. Phys.* **2005**, *123*, 244501.
(40) Schweizer, K. S.; Saltzman, E. J. *J. Chem. Phys.* **2004**, *121*, 1984–2000.
(41) Saltzman, E. J.; Schweizer, K. S. *J. Phys.: Condens. Matter* **2007**, *19*, 205123.
(42) Kirkpatrick, T. R.; Wolynes, P. G. *Phys. Rev. A* **1987**, *35*, 3072–3080.
(43) Novikov, V. N.; Sokolov, A. P. *Phys. Rev. E* **2003**, *67*, 031507.
(44) Eyring, H. *J. Chem. Phys.* **1936**, *4*, 283–291.
(45) Osborne, M. J.; Lacks, D. J. *J. Phys. Chem. B* **2004**, *108*, 19619–19622.
(46) Malandro, D. L.; Lacks, D. J. *J. Chem. Phys.* **1999**, *110*, 4593–4601.
(47) Warren, M.; Rottler, J. *Phys. Rev. E* **2007**, *76*, 031802.
(48) Kobelev, V.; Schweizer, K. S. *Phys. Rev. E* **2005**, *71*, 021401.
(49) Langer, J. S. *Phys. Rev. E* **2008**, *77*, 021502. **2004**, *70*, 041502. Langer, J. S.; Pechenik, L. *Ibid.* **2003**, *68*, 061507.
(50) Struik, L. C. E. *Physical Aging in Amorphous Polymers and Other Materials*; Elsevier: Amsterdam, 1978.
(51) Saltzman, E. J.; Schweizer, K. S. *J. Chem. Phys.* **2004**, *121*, 2001–2009.
(52) The PMMA compressibility and density data[40,51] above T_g yield the parameters $A \cong 0.693$ and $B \cong 1134$ K that quantify the equilibrium $S_0(T)$. Requiring the theory in the equilibrated supercooled state quantitatively reproduces[32] the typical experimental values of T_c (426 K) and T_g (378 K) for PMMA as defined by $\tau_\alpha(T_g) = 100$ s fixes $\rho\sigma^3 = 0.92$ and $a_c \cong 5$ in eq 4. In the glass state, the frozen density fluctuation parameter in eq 6 is fixed at $b = 2/3$, a value consistent with PMMA scattering experiments.[35] The statistical segment length is fixed at $\sigma = 1$ nm, a value that lies between the two classic estimates based on an equilibrium segment length and a Kuhn length.[37,38,41]

(53) Klompen, E. T. J.; Engels, T. A. P.; Govaert, L. E.; Meijer, H. E. H. *Macromolecules* **2005**, *38*, 6997–7008.
(54) Meijer, H. E. H.; Govaert, L. E.; Smit, R. J. M. A Multi-Level Finite Element Method for Modeling Rubber-Toughened Amorphous Polymers. In *Toughening of Plastics. Advances in Modeling and Experiments*; 2000; pp 50−70.
(55) Engels, T. A. P.; Govaert, L. E.; Meijer, H. E. H. *Macromol. Mater. Eng.* **2009**, *294*, 821–828.
(56) van Melick, H. G. H.; Govaert, L. E.; Meijer, H. E. H. *Polymer* **2003**, *44*, 3579–3591.
(57) Droger, N.; Primel, O.; Halary, J. L. *J. Appl. Polym. Sci.* **2008**, *107*, 455–462.
(58) Adijanto, E.; Lee, E.; Medvedev, G.; Caruthers, J. M., private communication.
(59) Riggleman, R.; Lee, H. N.; Ediger, M. D.; de Pablo, J. J. *Phys. Rev. Lett.* **2007**, *99*, 215501.
(60) Besseling, R.; Weels, E. R.; Poon, W. C. K. *Phys. Rev. Lett.* **2007**, *99*, 028301.
(61) Saltzman, E. J.; Yatsenko, G.; Schweizer, K. S. *J. Phys.: Condens. Matter* **2008**, *20*, 244129.
(62) Rottler, J.; Robbins, M. O. *Phys. Rev. Lett.* **2005**, *95*, 225504.
(63) Schweizer, K. S. *Curr. Opin. Colloid Interface Sci.* **2007**, *12*, 297–306. Saltzman, E. J.; Schweizer, K. S. *Phys. Rev. E* **2008**, *77*, 051504.
(64) Schweizer, K. S.; Saltzman, E. J. *J. Phys. Chem. B* **2004**, *108*, 19729.